Integrated Framework of DFT, Empirical potentials and Full Lattice Atomistic Kinetic Monte-Carlo to Determine Vacancy Diffusion in SiGe

Yong-Seog Oh
Synopsys Inc.
Mountain View, CA, USA
yso@synopsys.com

Yumi Park
Synopsys Inc.
Mountain View, CA, USA
yumip@synopsys.com

Christoph Zechner
Synopsys GmbH
Aschheim, Germany
zechner@synopsys.com

Ignacio Martin-Bragado
Synopsys Inc.
Mountain View, CA, USA
nacho@synopsys.com

***Abstract*—To simulate the point-defect diffusion in atomic scale, the software platform with a full lattice atomistic kinetic Monte-Carlo (AKMC) capability was developed. In this platform, the theoretical values of migration frequencies and barriers depending on the configuration of the nearest neighbors were automatically calculated by linking the simulator with the density functional theory (DFT) and classical molecular dynamics (CMD) tools. Ge mole fraction dependent diffusivity of a vacancy in SiGe was extracted in this work.**

Keywords—KMC, DFT, MD, vacancy, diffusivity, SiGe

I. INTRODUCTION

A DFT tool is widely used to compute the fundamental physical quantities such as the formation and migration vibrational frequencies and energies of defects. Doing such calculations for an alloy system is a formidable task because the total number of calculations can be huge (several thousand or more) and DFT tools are very sophisticated and fragile, and CPU expensive. A CMD tool can be used to provide the best initial guess for a DFT calculation. We have developed the software platform in which this complicated procedure was automated and its output was fed to the AKMC simulation. We calculated the Ge mole fraction dependent diffusivity of a vacancy in SiGe from this platform.

II. SOFTWARE PLATFORM

We have developed the software platform, Sentaurus Materials Workbench (SMW) [1], linking with CMD and DFT tool, QuantumATK [2], and implemented the automated flow to extract the diffusivity of a point-defect in an alloy system such as SiGe or in a compound material such as TiN. The flow consists of four major tasks: (1) creating defect systems and their structure optimizations, (2) creating initial migration paths and nudged elastic band (NEB) [3] calculations, (3) calculating vibrational frequency calculations, and (4) AKMC simulations and diffusivity extraction. The tasks must be executed sequentially. In this flow, SMW allows to combine CMD and DFT simulations so that CMD results are fed to DFT simulations as the initial atom positions, which improves the convergence speed of DFT simulation. SMW automates the flow so that all tasks are automatically created, scheduled, performed and monitored as shown in Fig.1.

A. Creating defect systems and structure optimizations

The defect systems are generated from the pristine system. SMW can generate an interstitial, a pair, and a cluster as well as a vacancy. Parameters such as lattice vectors, cutoff energy and k-points to optimize the structure inherit from ones for the pristine system except that the fixed volume condition is applied to the defect systems. SMW extracts the defect formation energy after the structure optimization, as in (1).

$$E_f = E_{tot} - E_{tot0} - \Sigma n_i \mu_i + q(E_F + \varepsilon_{VBM}) + \Delta E_{corr} \quad (1)$$

where E_{tot} and E_{tot0} are the total energies of the defect system and the pristine system respectively, n_i and μ_i are the number and chemical potential respectively of added or removed atoms of the atom species i, E_F and ε_{VBM} are the Fermi level relative to valence band maximum (VBM) and the eigen value of VBM respectively, and ΔE_{corr} is the energy to correct the effect due to too high defect concentration caused by a limited supercell size [4][5].

B. Creating initial migration paths and NEB calculations

The energy barrier for a defect to jump to an adjacent energetically favorable site is the migration energy. The NEB method can find such reaction path and energy. After structure optimization of the initial and final states on the reaction path, the linear interpolation between the initial and final states is widely used to create the intermediate structures, called *images*, along the path. However, such simple linear interpolation can make nonphysical short-bond pairs which result in the bad convergence in NEB calculation. SMW adjusts the migration path and neighbor atom positions so that the distances between the migrating atom and its neighbor atoms are not less than the sum of the atomic radii as shown in

the diagram, Fig.2. This improves the convergence of the NEB calculations.

C. Calculating vibrational frequencies

The vibrational frequencies at the initial and transition states of the migration path can be calculated by either CMD using empirical potentials or DFT using the density functional perturbation theory. The defect formation entropy is calculated by applying the harmonic approximation for partial vibrational frequency and the zone-center phonon frequencies [6].

D. AKMC simulation and diffusivity extraction

The probability of the defect formation at a specific local configuration is calculated as shown in (2).

$$P_j = exp((<S_{f,j}>T - <E_{f,j}>)/kT)/ \Sigma exp((<S_{f,j}>T - <E_{f,j}>)/kT) \quad (2)$$

where $<S_{f,j}>$ and $<E_{f,j}>$ are the average formation entropy and energy at the specific local configuration, *j*. k and T are the Boltzmann constant and the simulation temperature, respectively.

One defect is introduced at a random location in AKMC simulation domain according to the formation probability depending on a local configuration. The effective migration frequency is calculated with the vibrational frequencies at the initial state and the transition state by applying the transition state theory [7], as in (3).

$$\nu^* = \prod_i^N \nu_i \Big/ \prod_i^{N-1} \nu_i' \quad (3)$$

where $\{\nu_i\}$ and $\{\nu'_i\}$ are the phonon spectra of the initial and transition states respectively.

The jumping rate of a defect along the migration path from the start to end local configurations, *i* to *j* is given, as in (4).

$$R_{i\to j} = \nu^*_{i\to j} \, exp(-E_{m,i\to j}/kT) \quad (4)$$

where $E_{m,i\to j}$, is the migration energy to jump from *i* to *j* local configurations.

The diffusivity is calculated from the resultant of total jumping displacements after a given number of random jumps with the probabilities at a given temperature, as in (5). The AKMC simulator automatically extends the structure by attaching another domain when a moving atom crosses the domain border during simulation. For an alloy system, the extended structure is randomly alloyed.

$$D = \|\vec{r}_0 - \vec{r}_n\|^2/6t \quad (5)$$

where r_0 and r_n are the initial location and the final location after *n* jumps for time t.

To reduce the random fluctuation of D, the diffusivities for many samples with different random seeds are extracted and averaged, as in (6).

$$\langle D \rangle = \frac{1}{m}\sum_i^m \left\|\vec{r}_{0,i} - \vec{r}_{n,i}\right\|^2/6t_i \quad (6)$$

SMW executes AKMC simulations at different temperatures to get the data of T vs. <D> and extracts the diffusion constant and activation energy by fitting Arrhenius equation, as shown in Fig.3.

III. APPLICATION TO VACANCY IN SiGe

We applied SMW to extract the diffusivity of a vacancy in SiGe. For studying vacancy diffusion in SiGe, the tasks take into account 64 start positions for the vacancy, and 4 end positions per start position, resulting in 64 relaxations and about 200 NEB's, and 300 phonon calculations, depending on the randomness of the alloyed mixture. SMW supports automated generation and execution of the large number of DFT and CMD input files needed for each Ge mole-fraction system.

We used 64 atom $Si_{(1-x)}Ge_{(x)}$ super cells with x=0, 0.25,0.5,0.75 and 1.0 where Si and Ge atoms were randomly distributed. The vacancy defect systems were created by removing single Si or Ge atom from the 64-atom supercells. Formation energies and migration barriers were determined with DFT using the generalized gradient approximation (GGA) in the parametrization 'PBEsol' [8]. The k-point mesh was set to Γ−centered 3x3x3. The cell boundary for relaxations and NEB calculations was fixed to the same as the relaxed pristine supercell. The climbing image NEB method [9] was used to calculate the migration barrier.

To obtain the vibrational frequencies, we used CMD with Tersoff [10] empirical potentials, which is faster than the density functional perturbation theory.

In this work, we studied the diffusion of a vacancy in SiGe with AKMC along the following line, illustrated in Fig. 4. SMW extracts the migration barriers and frequencies of all possible vacancy jumps from the results of DFT NEB calculations and CMD phonon calculations. For the next step, all possible jumps in that supercell are divided into groups. Each group is defined by the jump conditions (a) the number of first nearest neighbor (1NN) Ge atoms at the original vacancy position, (b) the number of 1NN Ge atoms after the jump, and (c) the atom species (Si or Ge) which moves into the original vacancy position. The migration barriers in each group are averaged. SMW generates the table with the jump conditions vs. averaged migration barriers. This table is then used by the AKMC simulator to perform many jumps of a vacancy in a large SiGe crystal, for various temperatures. At any vacancy position, the event rate to jump into each of the

four 1NN positions is determined using this table. After each jump the arrangement of atoms in SiGe is updated accordingly. Simulations were repeated many times for accurate statistics. Diffusivities were extracted for each temperature. Finally, an Arrhenius expression was fitted to the temperature dependent diffusivities. AKMC simulations can be repeated for SiGe systems of many different Ge mole fractions.

IV. RESULTS AND DISCUSSIONS

The formation energies depend mainly on the number of Ge atoms located at 1NN lattice sites to the vacancy (Fig. 5). The more 1NN Ge atoms, the lower the formation energy of a vacancy. Since Ge atoms are larger than Si atoms, vacancy formation is easier at the sites surrounded by more Ge atoms. The activation energy of the effective vacancy diffusivity shows a concave dependency on Ge mole-fraction (Fig.6), which can be modeled by a quadratic polynomial. This indicates that an atom moves slower in unsymmetrical local configurations than in symmetrical ones. On the other hand, the Boltzmann-averaged formation energy of vacancies is dominated by the few most stable configurations and shows a convex dependency (Fig.7). Thus, the sum of activation and formation energies almost linearly depends on Ge mole fraction (Fig.8). For vacancy transport, only the product of diffusivity and equilibrium concentration ($D_V \cdot C_V$) can be reliably extracted from experiment. The measured energies of $D_V \cdot C_V$ in Si and Ge are 4.65±0.05 eV [11] and 3.13±0.03 eV [12], respectively. In comparison with the measurements, the calculations in this work underestimate them by about 1 eV, as shown at x=0 and 1 in Fig.8. This differences mainly result from the limited accuracy of defect formation energies predicted by the GGA PBEsol functional [13]. With a sufficiently powerful computing environment, more accurate results could be achieved with a hybrid functional, e.g. HSE06.

V. CONCLUSION

We developed the software platform to automate the flow from DFT and CMD to AKMC. The platform was applied to extract the Ge mole fraction dependent formation energy and diffusivity of a vacancy in SiGe. The activation energy of the vacancy diffusion in SiGe can be modeled with a concave quadratic polynomial equation with respect to the Ge mole fraction.

REFERENCES

[1] Sentaurus Materials Workbench O-2018.06, Synopsys Inc.

[2] QuantumATK 2018, Synopsys Inc.

[3] H. Jónsson, G. Mills, K. W. Jacobsen, "Nudged Elastic Band Method for Finding Minimum Energy Paths of Transitions, in Classical and Quantum Dynamics in Condensed Phase Simulations", Ed. B. J. Berne, G. Ciccotti and D. F. Coker, 385 (World Scientific, 1998)

[4] C. Freysoldt, J. Neugebauer, and C. G. Van de Walle, "Fully Ab Initio Finite-Size Corrections for Charged-Defect Supercell Calculations," Physical Review Letters, vol. 102, no. 1, p. 016402, January 2009

[5] Christoph Freysoldt, Blazej Grabowski, Tilmann Hickel, Jörg Neugebauer, Georg Kresse, Anderson Janotti, and Chris G. Van de Walle, "First-principles calculations for point defects in solids," Reviews of Modern Physics, vol. 86, no. 1, pp. 253–305, 2014

[6] P. Ágoston and K. Albe, "Formation entropies of intrinsic point defects in cubic In2O3 from first-principles density functional theory calculations," Physical Chemistry Chemical Physics, vol. 11, no. 17, pp. 3226–3232, 2009.

[7] G. H. Vineyard, "Frequency factors and isotope effects in solid state rate processes", J. Phys. Chem. Solids v.3, pp.121-127, 1957.

[8] J. P. Perdew, A. Ruzsinszky, G. I. Csonka, O. A. Vydrov, G. E. Scuseria, L. A. Constantin, X. Zhou and K. Burke, "Restoring the Density-Gradient Expansion for Exchange in Solids and Surfaces", Phys. Rev. Lett. 100, 136406, 2008.

[9] G. Henkelman and H. Jónsson, "A climbing image nudged elastic band method for finding saddle points and minimum energy paths", *J. Chem. Phys.* v.113, pp.9901-9904, 2000.

[10] J. Tersoff, "Modeling solid-state chemistry: Interatomic potentials for multicomponent systems", Phys. Rev. B, 39, 5566 , 1989.

[11] T. Südkamp and H. Bracht, "Self-diffusion in crystalline silicon: A single diffusion activation enthalpy down to 755°C", Phys. Rev. B 94, 125208, 2016.

[12] E. Hüger, U. Tietze, D. Lott, H. Bracht, D. Bougeard, E. E. Haller, and H. Schmidt. "Self-diffusion in germanium isotope multilayers at low temperatures", Appl. Phys. Lett. 93, 162104, 2008.

[13] Y. Park, C. Zechner, Y. Oh, H. Kim, I. Martin-Bragado, E. M. Bazizi and F. Benistant, "Dopant diffusion in Si, SiGe and Ge : TCAD model parameters determined with density functional theory", IEDM 2017

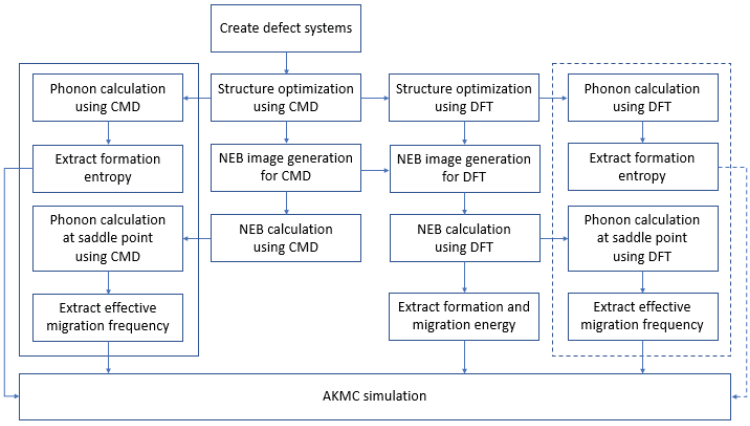

Fig.1. Automated flow to extract the diffusivity (Either phonon calculation using CMD in left solid box or phonon calculation using DFT in right dotted box can be chosen.)

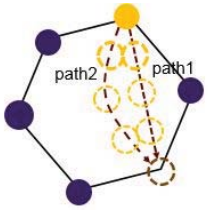

Fig.2. Diagram of the adjusted path for a vacancy jump to the second nearest neighbor (path1 and path2 show the linear interpolated path and the adjusted path respectively.)

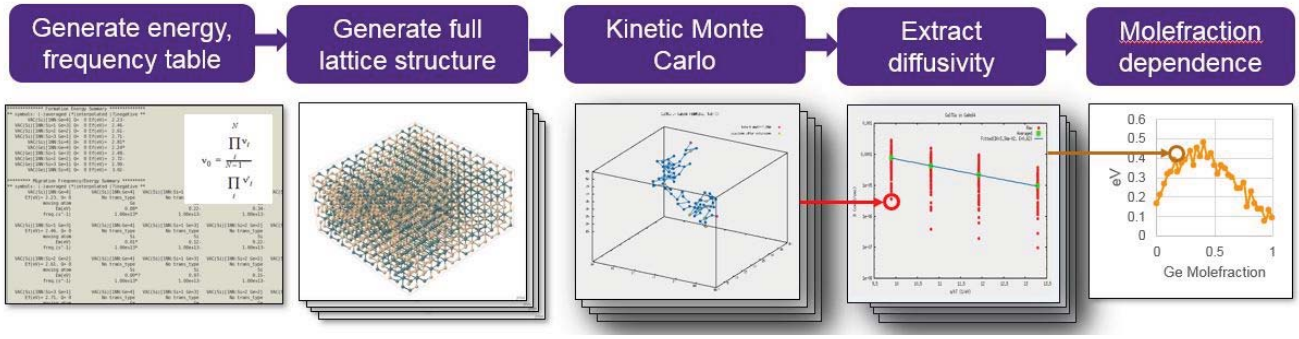

Fig.4. Automated flow of AKMC simulation for Ge mole fraction dependence extraction

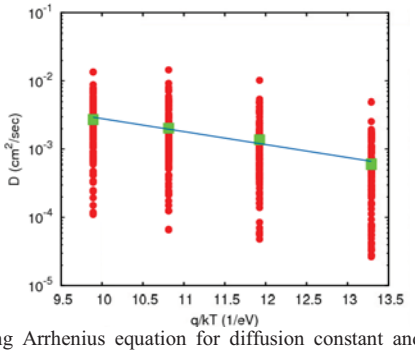

Fig.3. Fitting Arrhenius equation for diffusion constant and activation energy (red dot: D, green box: <D>, line: Arrhenius equation fit.)

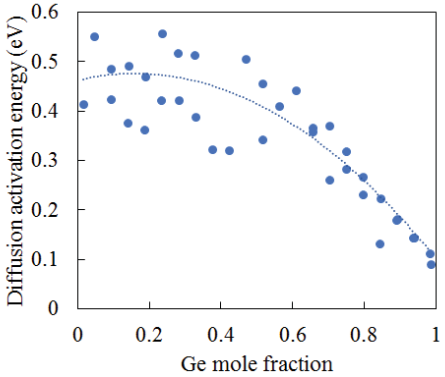

Fig.6. Diffusion activation energy of a vacancy in $Si_{(1-x)}Ge_{(x)}$

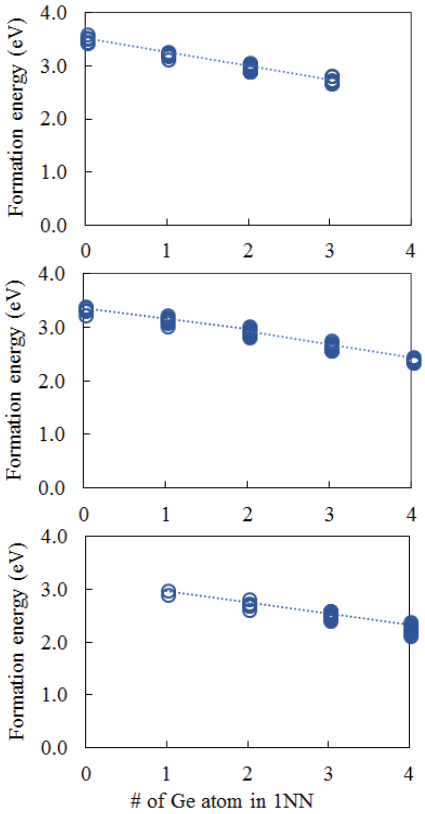

Fig.5. Dependence of vacancy formation energy on number of 1NN Ge atoms in $Si_{0(1-x)}Ge_{(x)}$ for x=0.25,0.50,0.75 from top to bottom

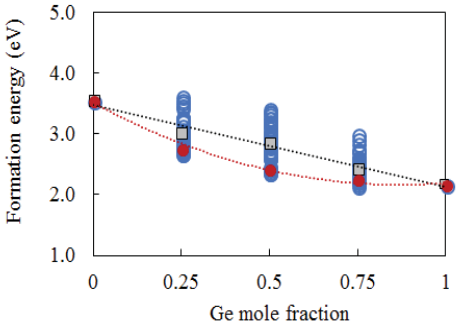

Fig.7. Vacancy formation energy in $Si_{(1-x)}Ge_{(x)}$ (empty circle: raw data, filled circle: Boltzmann average, box: simple average)

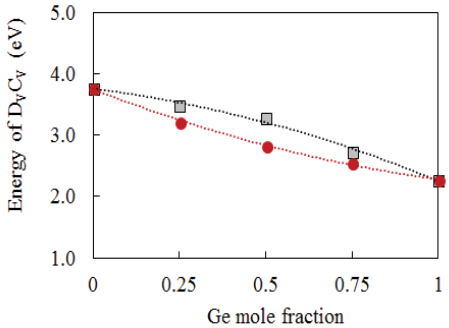

Fig.8. Energy of the product of diffusivity and equilibrium concentration of a vacancy in $Si_{(1-x)}Ge_{(x)}$ (filled circle: Boltzmann average, box: simple average)